Highlights

An efficient low-delay polyphase implementation method for active noise control systems

Yongjie Zhuang, Yangfan Liu

- A filter implementation structure designed for delay-sensitive applications
- The real-time computations that increase with the sampling rate are reduced from quadratic to linear
- Significant noise control performance enhancement compared with traditional methods

This manuscript was published in Applied Acoustics.

DOI: https://doi.org/10.1016/j.apacoust.2024.110232

An efficient low-delay polyphase implementation method for active noise control systems

Yongjie Zhuang[a,b], Yangfan Liu[a]

[a] *Ray W. Herrick Laboratories, Mechanical Engineering, Purdue University, 177 S Russell St, West Lafayette, 47907, Indiana, USA*
[b] *Electrical and Computer Engineering, Stony Brook University, Light Engineering Lab, Stony Brook, 11794, New York, USA*

Abstract

When implementing active noise control systems on signal processing hardware, the time delay introduced by electronic components (especially components requiring additional lowpass filters or introducing fixed-sample-size delays) may adversely affect the noise control performance. One common approach to reducing this delay is to use a high sampling rate, but this increases the computation significantly when implementing the ANC filters in real time. In the current work, a polyphase-structure-based filter design method is developed for active noise control systems that can reduce the computation load for real-time filter implementation but do not introduce an additional time delay. Although the computation reduction capability of a polyphase filter structure is well known for multi-rate systems, the traditional use of such multi-rate systems requires additional anti-aliasing and reconstruction filters which introduces an additional time delay. Thus, in delay-sensitive applications, such as active noise control, this method was previously applied only on the filter adaption phase, instead of directly on the real-time filtering process. In this article, a filter decomposition method using the minimum-phase technique is proposed to decompose an ANC filter into two multiplicative causal filters both of which have lowpass frequency response shapes at high frequencies such that the polyphase structure can be applied directly to the two multiplicative causal control filters without introducing additional anti-aliasing and reconstruction filters. Results show that, compared with various traditional low sampling rate implementations, the proposed method

Email address: Corresponding author: yangfan@purdue.edu (Yangfan Liu)

can significantly improve the noise control performance. Compared with the non-polyphase high-sampling rate method, the real-time computations that increase with the sampling rate are improved from quadratically to linearly.

Keywords: active noise control, polyphase method, multi-rate signal processing, efficient filter implementation, minimum phase filter, constrained filter design

---

1. Introduction

Active noise control (ANC) is a technique where control filters are designed to process the sensor signals and control secondary sources to produce anti-noise waves that interfere with original primary noise waves destructively. In recent decades, because of the development of computing devices, e.g., the digital signal processor and FPGA, ANC technologies were successfully applied to a wide range of applications, such as headrests [1, 2], headphones [3, 4, 5], automobiles [6, 7], open windows [8], etc.

For practical active noise control (ANC) applications, most of the control systems are realized by digital control systems. When digital control systems are implemented, an electronic delay will be introduced into the signal path because of the anti-aliasing and reconstruction filters in the analog-to-digital converters (ADC) and digital-to-analog converters (DAC) [9, 10, 11]. The electronic delay can be a critical problem in ANC systems [12], especially for broadband systems, which adversely affects the noise control performance, and causes causality problems in filter design [13].

Increasing the sampling rate of the digital system [10, 12] is an effective and common way to reduce electronic delay since the group delay in anti-aliasing and reconstruction filters decreases with the sampling interval linearly [14]. The group delay in anti-aliasing and reconstruction filters can be reduced or even removed [9] if the cut-off frequency is much higher [12, 15]. Also, for sigma-delta type ADC, there will be a delay of a fixed number of samples and a higher sampling rate will result in a shorter time delay. However, increasing the sampling rate will significantly increase the required real-time computations. The required order of the control filter will be increased proportionally to the sampling rate if the filters' effective time lengths, i.e., the impulse response duration in time are kept the same. Also, each output signal sample needs to be computed in a shorter sampling interval for a higher sampling rate. Thus, the required real-time multiplications

per second will usually increase quadratically with the sampling rate.

One commonly used approach to improving the real-time computational efficiency of high sampling rate ANC systems is to use a multi-rate system with a polyphase filter structure so that the sampling rate for implementing control filters is relatively lower than the sampling rate of the input and output signals [16, 17, 18, 19]. However, the use of a multi-rate system requires additional lowpass filters (anti-aliasing and reconstruction filters) which also introduce additional delay in real-time implementation. Thus, in ANC applications, the multi-rate techniques with polyphase structures were only applied in the filter adaption process instead of the real-time filtering process, e.g., the subband ANC method [16, 17]. This additional lowpass filter-induced delay contradicts the purpose of using a high sampling rate to reduce the electronic delay, thus, the traditional delayless subband ANC techniques cannot be used to improve the real-time computational efficiency in the real-time active noise control filtering process.

In this article, an efficient low-delay polyphase real-time ANC filter implementation method without the need for additional lowpass filters is proposed. The key step involves a new method to decompose an ANC filter into two multiplicative causal filters both of which have lowpass frequency response shapes at high frequencies. More specifically, the proposed method uses the fact that, for high sampling rate ANC systems, the frequency responses of the designed ANC filter should be attenuated to prevent noise amplification outside the desired noise control band (usually the desired noise control band is at low frequencies). The ANC filter's attenuation at higher frequencies can be used as anti-aliasing and reconstruction filters if the proposed causal filter decomposition is applied. Then, a polyphase filter structure can be implemented without additional anti-aliasing and reconstruction filters. By using the proposed method, an ANC system can be operated at a sampling rate much higher than the desired frequency band. Compared with traditional direct filter implementation, the associated real-time computation requirement using the proposed method only increases linearly with the sampling rate instead of quadratically. When the ANC system is operated at a high sampling rate, the introduced electronic delay will be lower, and better noise control performance can be achieved. Experiments are implemented to confirm the improvement of real-time computations and noise control performance compared with various traditional implementations. A smaller delay can also allow broadband ANC techniques to be applied to wider space-limited applications because it allows a smaller distance between the reference sensors

and the actuators, and a smaller distance between the reference sensors and the error sensors.

2. Theory

In this section, the discussion is based on single-channel active noise control systems. The extension of the proposed method to multi-channel systems is trivial since the proposed method can be applied channel by channel independently. The discussion focused only on the fixed-coefficient controller case (i.e., non-adaptive filter) because the proposed method is applied directly to the real-time filter implementation process and reduces the real-time computational effort, instead of to the filter coefficients adaption process where the polyphase method is traditionally used in previous studies [16, 17]. Moreover, the fixed-coefficient controller is becoming the de facto approach in most commercial digital ANC products [13]. For time-varying environment, selective fixed-filter ANC can be used, i.e., multiple non-adaptive filters are trained before real-time implementation and are selected during real-time implementation [13, 20, 21]. Thus, the proposed method explained in this section will be discussed on fixed-coefficient controller cases and can be directly applied to either fixed-coefficient ANC applications or selective fixed-filter ANC applications for a time-varying environment. For practical consideration, filter coefficients are real-valued numbers in this article.

2.1. Review of Traditional ANC system and Polyphase Implementation

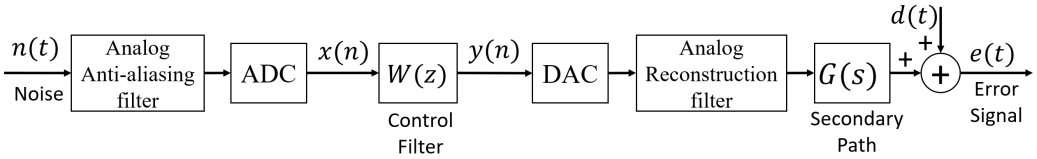

Figure 1: Block diagram of the commonly used implementation of fixed-filter ANC digital controllers.

The system block diagram of a typical ANC controller is shown in Fig. 1. $n(t)$ represents the analog noise signal from noise sources. $x(n)$ represents the sampled reference signal. $W(z)$ is the designed digital ANC FIR filter. $y(n)$ is the digital output signal. The secondary path $G(s)$ represents the acoustical responses of the secondary source at the error sensor positions.

$d(t)$ is the disturbance signal to be controlled by the signal produced by the secondary source. $e(t)$ is the error signal whose power is to be minimized when designing the control filter coefficients.

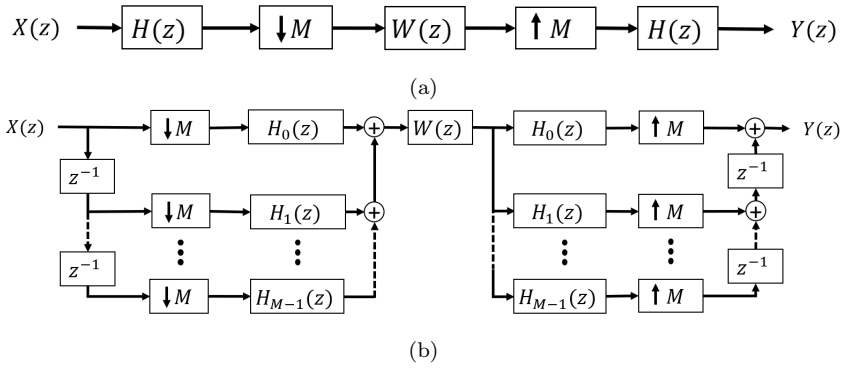

Figure 2: Block diagrams of (a) a typical multi-rate system, (b) a multi-rate system after applying polyphase filter structures.

While the desired noise control band is still at the low-frequency band, the sampling rate can be increased to reduce the delay introduced by anti-aliasing and reconstruction filters, ADC, and DAC [12, 15], i.e., $X(z)$ in Fig 1 is at a high sampling rate. To reduce the real-time computations, a multi-rate system can be applied. In Fig. 2 (a), a block diagram of a commonly used multi-rate system is shown. $X(z)$ is the digital signal sampled at a sampling rate of f_s. $H(z)$ is a lowpass filter with a cutoff frequency at f_c. If $H(z)$ is assumed to be an ideal lowpass filter and $f_s/f_c > 2M$, then a downsampling with a decimation factor of M can be achieved without aliasing. $W(z)$ is a digital filter (the designed ANC filter) that will be implemented with a sampling rate of f_s/M. The real-time computations in $W(z)$ will then be reduced to $1/M$ of the computations to achieve the same impulse response, compared with implementing the filter at a sampling rate of f_s. However, the lowpass filter $H(z)$ is still operated at the higher sampling rate, f_s.

To further reduce the real-time computations in implementing $H(z)$, polyphase implementation can be applied. In Fig. 2 (b), the traditional use of a polyphase filter structure is illustrated. $H(z)$ can be expressed as

$$H(z) = h_0 + h_1 z^{-1} + h_2 z^{-2} + \ \ldots \ + h_{L-1} z^{-L+1}. \tag{1}$$

If a proper choice of filter length or zero-padding of the filter length is applied, it is always possible to have the ratio of the filter length to decimation factor,

$P = L/M$, to be an integer. Then the lowpass filter $H(z)$ can be split into multiple filter phases, $H_m(z)$:

$$H_m(z) = \sum_{n=0}^{P-1} h_{nM+m} z^{-n}. \tag{2}$$

According to the first and second noble identities [22], if $X(z)$ are the same for the two filter structures in Fig. 2 (a) and (b), $Y(z)$ will also be the same for the two filter structures. Compared with Fig. 2 (a), the filter structure in Fig. 2 (b) performs the downsampling operation before any filters are applied and upsampling operation after all filters are applied. Thus, the filter structure in Fig. 2 (b) reduces the real-time computations both in $H_m(z)$ (or essentially the $H(z)$) and $W(z)$. Similarly, the lowpass filter $H(z)$ can be replaced by other band-limited sub-band filters so that signals content in each associated frequency band can be processed separately. More details of multi-rate polyphase filter structure can be referred to Chapter 11 in Proakis and Manolakis' book [22].

The use of a multi-rate system with polyphase filter structure implementation can reduce the high real-time computations caused by a high sampling rate. And this high sampling rate in input signal $X(z)$ and output signal $Y(z)$ will allow a lower delay in the analog anti-aliasing and reconstruction filters as well as ADC and DAC hardware. However, because of the downsampling and upsampling operations, two lowpass filters $H(z)$ are always required, which inevitably introduce additional time delay to the system compromising the performance if the application is delay sensitive (e.g., active noise control application).

2.2. Proposed Efficient Low-Delay Polyphase Implementation Design

As mentioned in the Introduction Section, in broadband ANC applications, although the desired noise control is focused on the relatively low-frequency content, it is still desirable to use a higher sampling rate to reduce time delay [12, 15] introduced by electronic components (anti-aliasing and reconstruction filters, ADC, and DAC) so that better noise control performance can be achieved. The associated trade-off is the higher real-time computational efforts resulted from the use of a high sampling rate [12]. Although the traditionally used polyphase filter structure in multi-rate systems can reduce the real-time computations significantly, the lowpass filters $H(z)$ are required as additional digital anti-aliasing and reconstruction filters when

performing upsampling and downsampling operations. Those lowpass filters will introduce an additional delay in real-time signal processing, which will degrade the control performance in delay-sensitive applications such as ANC applications, especially for broadband active noise control. Thus, multi-rate and polyphase implementation is usually used only for the filter adaption process (e.g., at LMS part) in ANC applications which is known as delayless subband ANC techniques [16, 17]. The real-time computation of the filtering process still remains high.

In this section, an efficient low-delay polyphase implementation is proposed which can be applied directly to the real-time filtering process to reduce the real-time computations without introducing additional delay caused by additional digital anti-aliasing and reconstruction filters $H(z)$. The proposed method is stated as the following.

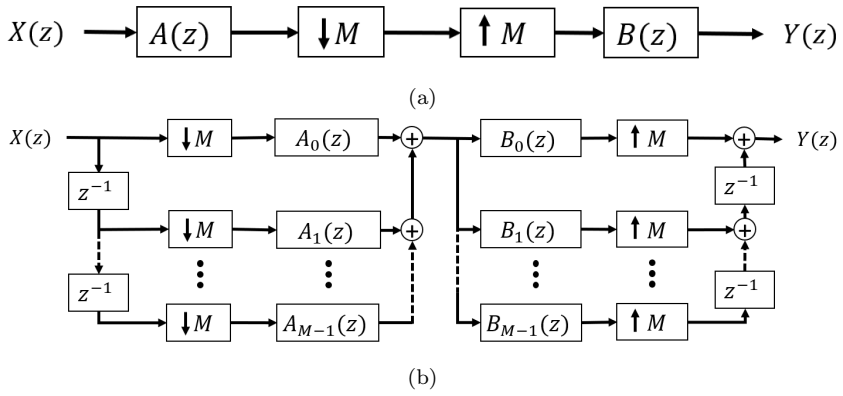

Figure 3: Block diagrams of (a) a proposed ANC filter structure that $H(z)$ is replaced by $A(z)$ and $B(z)$ and no $W(z)$ is required, (b) a proposed ANC filter structure after applying polyphase filter structures.

The purpose is to use a polyphase structure to reduce the real-time computation load to implement the ANC filter, $W(z)$, that is designed at a high sampling rate $f_H = Mf_L$ where M is the decimation factor when a multi-rate system is used to implement this filter. The desired noise control band is below $f_L/2$. In the filter design process (using a high sampling rate f_H), the response of $W(z)$ at frequencies above $f_L/2$ can be arbitrary as long as it provides sufficient attenuation to prevent noise amplification outside the desired noise control frequency band. In this way, the ANC filter $W(z)$ can actually perform as a lowpass filter with cut-off frequency at $f_L/2$. An ANC

filter that satisfies the above-mentioned requirements can be designed by the constrained optimization method formulated using the convex cone programming [23, 24]. After the FIR filter $W(z)$ is designed, it can be decomposed as

$$W(e^{j2\pi f}) = A(j2\pi f)B(j2\pi f), \quad \text{for } f < f_L/2, \tag{3}$$

where the responses of both $A(z)$ and $B(z)$ provide sufficient attenuation above $f_L/2$ (the approach to finding such a pair of $A(z)$ and $B(z)$ is discussed in the Section 2.3). Then $A(z)$ and $B(z)$ can be used to replace the two lowpass filters, $H(z)$, in Fig. 2 (a) and there is no need to have $W(z)$. A demonstration of this concept is shown in Fig. 3 (a). Similarly as in the traditional polyphase implementation, $A(z)$ and $B(z)$ can be expressed as:

$$\begin{aligned} A(z) &= a_0 + a_1 z^{-1} + a_2 z^{-2} + \ \ldots \ + a_{L_a-1} z^{-L_a+1}, \\ B(z) &= b_0 + b_1 z^{-1} + b_2 z^{-2} + \ \ldots \ + b_{L_b-1} z^{-L_b+1}. \end{aligned} \tag{4}$$

Then, let $P_a = L_a/M$ and $P_b = L_b/M$ (P_a and P_b are integers), $A_m(z)$ and $B_m(z)$ can be defined as:

$$\begin{aligned} A_m(z) &= \sum_{n=0}^{P_a-1} a_{nM+m} z^{-n}, \\ B_m(z) &= \sum_{n=0}^{P_b-1} b_{nM+m} z^{-n}. \end{aligned} \tag{5}$$

By the first and second noble identities [22], if $X(z)$ in Fig. 3 (a) and (b) are the same, $Y(z)$ will also be the same. In Fig. 3 (b), X(z) and Y(z) are still at higher sampling rate f_H and no additional delay is introduced into the signal path, so the noise reduction performance will not be adversely affected. However, at each sampling interval $1/f_H$, only one portion of A(z) and B(z) are computed which leads to the reduction of computational load. Figure 3 (b) is the proposed efficient low-delay polyphase implementation. Obviously,

$$Y(e^{j2\pi f}) = B(e^{j2\pi f})A(e^{j2\pi f})X(e^{j2\pi f}) = W(e^{j2\pi f})X(e^{j2\pi f}), \quad \text{for } f < f_L/2. \tag{6}$$

Thus, $A(z)$ and $B(z)$ can then perform both as the control filters in the lower frequency band (desired noise control band) and as the lowpass filters in the higher frequency band. No additional delay is introduced when using the

proposed efficient low-delay polyphase implementation since no additional lowpass filters are added. The real-time computations are also significantly reduced because the downsampling is operated before implementing filters and the upsampling is operated after using the filters.

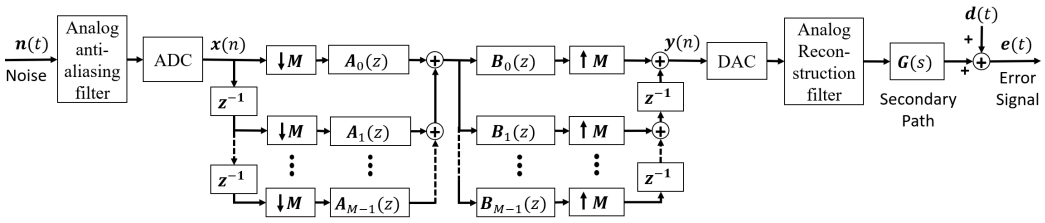

Figure 4: Block diagram of the ANC controllers when using the proposed efficient low-delay polyphase implementation.

The use of the proposed efficient low-delay polyphase implementation in ANC applications is then shown in Fig. 4. The delay introduced by the analog anti-aliasing and reconstruction filters, ADC, and DAC can be significantly reduced by using a high sampling rate for $x(n)$ and $y(n)$. The real-time computations are also significantly reduced because all digital filters are applied after the downsampling operation and before the upsampling operation. And no additional delay is introduced because there is no need for additional digital anti-aliasing and reconstruction filters. The comparison of real-time computations for various methods is listed in Table 1. When the low sampling rate method is used, the introduced delay will be high due to high delay in anti-aliasing and reconstruction filters, ADC, and DAC [12, 15], although the real-time multiplications per second will be relatively lower, i.e., the product of multiplications per sampling interval and sampling intervals per second: $Tf_L \times f_L = Tf_L^2$, where T is the effective time lengths (i.e., the impulse response duration) and f_L is the low sampling rate. To reduce the introduced delay, the sampling rate can be increased to Mf_L (M is an integer larger than 1) by redesigning the ANC filter using a higher sampling rate with constraints on the responses' magnitude above the desired noise control band using constrained optimization methods such as the convex conic formulation [23, 24]. And the impulse response duration T should be kept the same since the noise signal and transfer path are essentially analog (a direct implementation of this high sampling rate filter is referred to as the high sampling rate method). However, if the high sampling rate method is used, it increases the number of multiplications required per second to $T(Mf_L)^2 = M^2Tf_L^2$,

which is a quadratic growth with respect to M. To mitigate such a significant increase in computation load, the filter's impulse response duration, T, can be shortened (e.g., from T to T/M), this method is referred to as the high sampling rate method using shorter impulse response duration in the current work. In this method, the real-time multiplications per second are increased to MTf_L^2, which is a linear growth of sampling rate but the noise control performance is negatively impacted due to the shorter filter response time. By using the proposed method, suppose the total impulse response duration of designed $A(z)$ and $B(z)$ is αT, where α, depending on the filter decomposition method (introduced in Section 2.3), can be chosen to be 1 or sometimes slightly larger than 1 in practice. The real-time multiplications of the proposed method are then αMTf_L^2, which is also a linear growth of sampling rate, and the filter length is not shortened (i.e., the noise control performance is not degraded).

Table 1: A comparison of real-time multiplications per second for different traditional methods and the proposed method.

Methods	Low f_s method	High f_s method, original impulse response duration	High f_s method, shorter impulse response duration	Proposed method
Sampling Rate f_s	f_L	Mf_L	Mf_L	Mf_L
impulse response duration	T	T	T/M	$\alpha T^\star$
Filter Order	Tf_L	MTf_L	Tf_L	αMTf_L
Real-time Multiplications	Tf_L^2	$M^2Tf_L^2$	MTf_L^2	αMTf_L^2
Real-time Computational Complexity	$\mathcal{O}(1)$	$\mathcal{O}(M^2)$	$\mathcal{O}(M)$	$\mathcal{O}(M)$
Delay	High	Low	Low	Low

* α, depending on the filter decomposition method (introduced in Section 2.3), can be chosen to be 1 or sometimes slightly larger than 1 in practice.

2.3. Proposed Filter Decomposition Method

A key step of the proposed efficient low-delay polyphase implementation described in the previous subsection is to find a pair of suitable multiplicative decomposition of the designed ANC control filter $W(z)$ into two causal filters $A(z)$ and $B(z)$. There are three challenges in finding such a pair of filters:

1. The order of $W(z)$ is usually very high (e.g., several hundred) because the control filter is designed using a high sampling rate, this makes the dimension of the filter decomposition problem very high as well, which is not solvable by "brutal force" optimization approach (particle swarm optimization, genetic algorithm, etc.) within a practical computational time constraint. For example, for an ANC filter of order 300, by using the concept of evenly dividing FIR filter (polynomial) zeros into two multiplicative filters, up to $\frac{1}{2}C(300, 150) = \frac{300!}{2\times 150!\times(300-150)!} \approx 4.7\times 10^{88}$ local minimums exist, which makes the global minimum (or a usable local minimum) difficult to be found when high frequency constraints are considered.
2. The response of both $A(z)$ and $B(z)$ should have sufficient attenuation in frequency response above f_L to remove the need for anti-aliasing and reconstruction filters in traditional polyphase applications. Without this attenuation requirement, the decomposition of $W(z)$ into $A(z)$ and $B(z)$ can be achieved by simply obtaining the zeros of $W(z)$ and splitting the zeros into two groups for $A(z)$ and $B(z)$ (although the high order still poses numerical difficulties in the root-finding process [25]). This high-frequency response constraint also significantly increases the computational complexity if a "brutal force" optimization method is used to solve $A(z)$ and $B(z)$ from $W(z)$.
3. Both $A(z)$ and $B(z)$ must be causal so they can be implemented in a real-time delay-sensitive system such as an ANC system. Thus, simple frequency-domain fitting methods, such as fitting the square-rooted frequency responses of $W(z)$, cannot be used, because the causality of the resulting filters cannot be guaranteed.

To overcome the three challenges mentioned above, a filter decomposition method is proposed as the following. If the required attenuation for the stop bands of $A(z)$ and $B(z)$ is K dB, the ANC filter $W(z)$ is specified to have a $2K$ dB attenuation in this stop band during the optimal ANC filter $W(z)$ design process (this design specification can be achieved by methods

described in [23, 24]), i.e.,

$$20\log_{10}|W(e^{j2\pi f})| < -2K, \quad \text{for } f > f_L/2. \tag{7}$$

To perform the proposed decomposition, a minimum-phase lowpass filter $A(z)$ is firstly designed with a cut-off frequency $f_L/2$ where the stop band has K dB attenuation with stop band ripples of δ_s dB, i.e.,

$$-K - \delta_s < 20\log_{10}|A(e^{j2\pi f})| < -K + \delta_s, \quad \text{for } f > f_L/2. \tag{8}$$

Because $A(z)$ is a minimum-phase filter, $\frac{1}{A(z)}$ is also a minimum-phase filter, i.e., $\frac{1}{A(z)}$ is causal and stable. Since $W(z)$ is a designed FIR filter for ANC application which is always stable (having zeros only) and causal, it is easy to see that $\frac{W(z)}{A(z)}$ is causal and stable as well. A causal filter $B(z)$ can then be constructed by fitting the frequency responses of $\frac{W(z)}{A(z)}$, e.g., using least square approximation. Due to stop-band attenuation specifications for $W(z)$ and $A(z)$ listed above, it is obvious that

$$20\log_{10}|B(e^{j2\pi f})| \approx 20\log_{10}\left|\frac{W(e^{j2\pi f})}{A(e^{j2\pi f})}\right| < -K + \delta_s, \quad \text{for } f > f_L/2. \tag{9}$$

Thus, both $A(z)$ and $B(z)$ are attenuated as required above $f_L/2$, if a small enough ripple δ_s is chosen. Also, $A(e^{j2\pi f})B(e^{j2\pi f}) \approx W(e^{j2\pi f})$ for $f < f_L/2$. So the proposed filter decomposition method can indeed give a pair of suitable $A(z)$ and $B(z)$ for the proposed efficient low-delay polyphase implementation described in the previous subsection.

Figure 5 is a flow chart showing the procedure of using three traditional methods (i.e., the low sampling rate method, the high sampling rate method using original impulse response duration, or shorter impulse response duration) and the proposed efficient low-delay polyphase implementation along with the proposed causal filter decomposition method. When using traditional methods, it can only result in either less computational time or better noise control performance (but not both). However, if the proposed implementation is used, both the advantages of less real-time computations and better noise control performance can be achieved. This reduced delay can also enable a possibility for broadband ANC in space-limited applications with a reasonable real-time computation requirement.

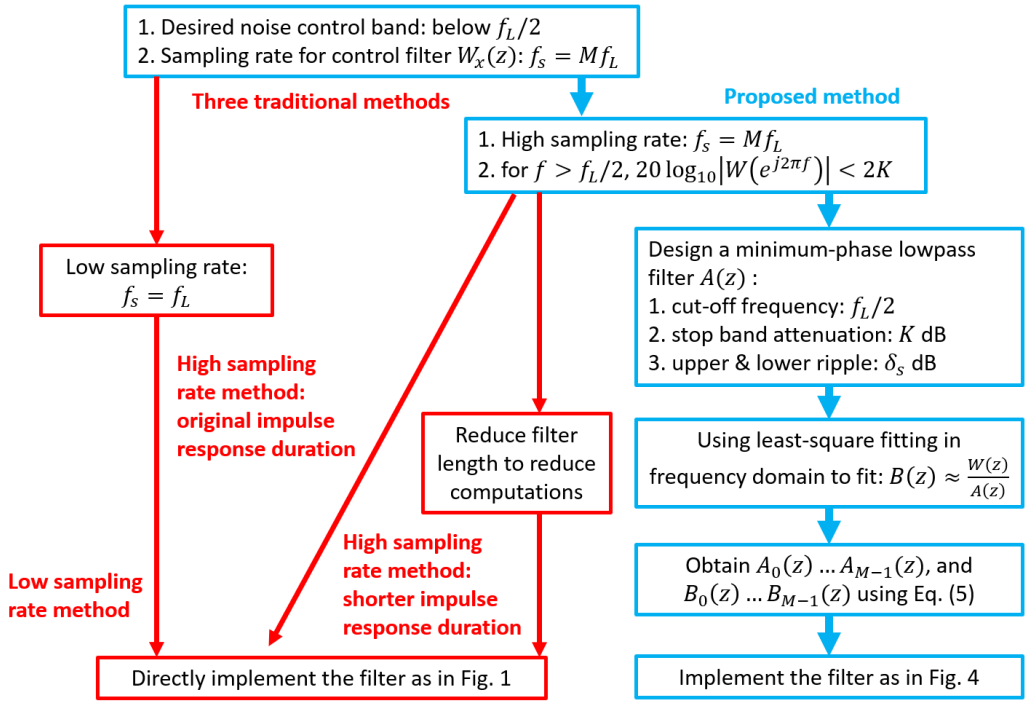

Figure 5: A flow chart showing the traditional filter implementation methods and the proposed ANC filter implementation method using efficient low-delay polyphase implementation.

3. Experimental Result

3.1. Experimental Setup

To investigate the performance of the proposed efficient low-delay polyphase implementation in ANC application, an installed single-channel ANC system is shown in Fig. 6. The dSPACE MicroLabBox is used as the real-time controller. Since, if a multi-channel system is involved, the proposed method can be applied channel by channel, demonstration using a single-channel ANC system is sufficient to investigate the performance of the proposed method. The primary noise source is a loudspeaker that plays a low-pass filtered white noise with a cut-off frequency of 9 kHz. The desired noise control frequency band is below $f_L/2 = 2$ kHz (i.e., the f_L defined in Section 2.2 is 4 kHz). Since the highest frequency component of the noise source signal (9 kHz) is much higher than the desired noise control frequency band (which is a very common case for most practical ANC applications), anti-aliasing fil-

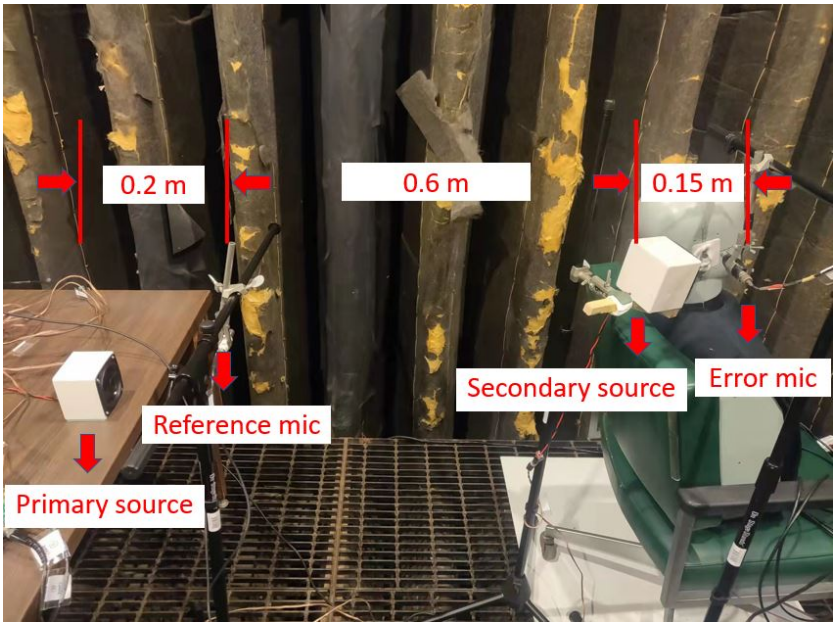

Figure 6: A picture of the experimental setup.

ters are usually needed to prevent aliasing. The secondary source is another speaker that produces the desired sound signal to reduce noise at the error microphone position. The relative difference in distance between the primary path (reference microphone to error microphone) and the secondary path (secondary source to error microphone) is approximately 0.6 meters, which means the introduced electronic delay (including the delay in anti-aliasing and reconstruction filters) should be less than 1.8 ms to form a feed-forward system for broadband noise control.

In this experimental setup, to more accurately set the control variables in high and low sampling rate cases, digital anti-aliasing and reconstruction filters, instead of analog filters, are implemented using a 20 kHz sampling rate. The cutoff frequency of anti-aliasing and reconstruction filters is 2 kHz for the low sampling rate (controller operates at 4 kHz) case and 10 kHz for the high sampling rate (controller operates at 20 kHz) case. The 20 kHz sampling rate is higher than twice of 9 kHz so a digital filter can be used to simulate analog anti-aliasing filters with better control over system parameters. For both high and low sampling rate cases, 1 dB ripple is allowed at the passband, and 30 dB attenuation in magnitude ($K = 30$ in Eq. (8)) is required for the stopband of the anti-aliasing and reconstruction filters. A

minimum order Butterworth filter [26] is used to design the anti-aliasing and reconstruction filter. The total electronic delay for the desired noise control band including group delay of anti-aliasing and reconstruction filter, and one-sample delay for the processing in controllers is shown in Fig. 7. From Fig. 7, the introduced electronic delay when using a low sampling rate controller (4 kHz) is higher than 2 ms, which is much higher than the high sampling rate case (the delay introduced in 20 kHz sampling rate case is less than 0.06 ms). As mentioned earlier, the relative difference in distance between the primary path (reference microphone to error microphone) and the secondary path (secondary source to error microphone) is approximately 0.6 meters, leading to a maximum delay limit of 1.8 ms to form a feed-forward system for broadband noise control. Thus, the low sampling rate controller case should not perform well which will also be confirmed in the later section.

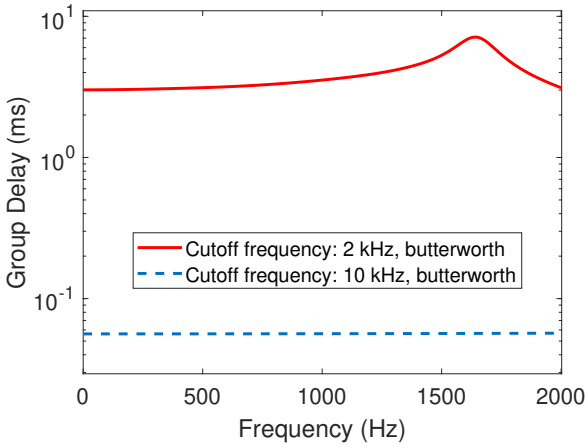

Figure 7: The total electronic delay including group delay of anti-aliasing and reconstruction filters, and one-sample delay for the processing in the ANC controller for two different sampling rates.

3.2. Comparison of noise control performance

The ultimate goal of reducing delay is to achieve better noise control performance. Thus, this section will compare the noise control performance at the desired noise control frequency band (below 2 kHz) by using various high sampling rate controller (20 kHz) methods (including the proposed method) and the low sampling rate controller (4 kHz) method. Besides lower delay, another main contribution of the proposed method is to reduce the real-time

computation complexity from quadratic to linear with the increase of sampling rate. In this section, the exact number of real-time multiplications will be compared between the proposed method and traditional high sampling rate controller methods for the specific experimental setup.

The noise control performance of using various traditional methods that directly implement the ANC filter as in Fig. 1 and the proposed method that implements the filter as in Fig. 4 are compared. For the high sampling rate controller (20 kHz) case, since the designed ANC filter response should be attenuated for at least 2K dB (in this experimental setup, the K in Eq. (7) is 30) above the desired noise control frequency band (2 kHz), the optimal ANC filter $W(z)$ is designed by the constrained optimization method developed by Zhuang and Liu [23, 24]. Two different choices of impulse response duration (15 ms and 3 ms) are used to design the ANC FIR filter. The 15 ms impulse response duration is chosen to be sufficiently long for this experimental setup. When impulse response duration T is 15 ms, the number of FIR ANC filter coefficients is 60 if the sampling rate is 4 kHz. However, the number of FIR filter coefficients reaches 300 if the sampling rate is 20 kHz which is significantly larger than 60 (i.e., $M = 5$). For the 20 kHz sampling rate, if the filter impulse response duration is reduced to 3 ms, the FIR ANC filter order is then the same as the 15 ms impulse response duration in a low sampling rate case.

To use the proposed method, two subfilters $A(z)$ (filter order 40) and $B(z)$ (filter order 300) are obtained by using the proposed filter decomposition method. Thus, α in Table 1 is 1.13 in this case. Using filter order 40 in $A(z)$ is sufficient to design a well-performed low-pass filter. Filter order 300 for $B(z)$ is used to make α around 1 for a fairer comparison with other traditional methods. In practice, this filter order can be either increased or decreased based on a tradeoff between real-time computations and noise control performance. Their frequency responses are shown in Fig. 8. From Fig. 8(a), the designed $A(z)$ and $B(z)$ using the proposed filter decomposition method have frequency responses well attenuated (K = 30 dB attenuation) above 2 kHz, which means that they can be used as anti-aliasing and reconstruction filters. From Fig. 8(b), it clearly shows that $A(e^{j2\pi f})B(e^{j2\pi f}) \approx W(e^{j2\pi f})$ below 2 kHz, which means that the decomposed $A(z)$ and $B(z)$ together can achieve the same noise control performance compared with using $W(z)$ in the desired noise control band (below 2 kHz).

Figure 9 confirms that the noise control performance of using the proposed method has no observable difference from the performance achieved

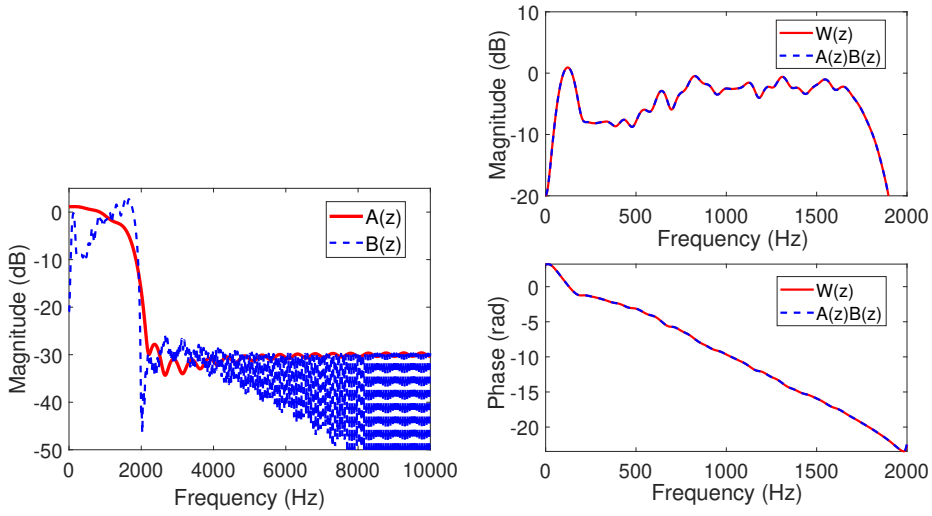

(a) (b)

Figure 8: (a) Magnitude of the frequency responses of $A(z)$ and $B(z)$ for the whole frequency band to show they are well attenuated above 2 kHz, (b) comparison of magnitude and phase of the frequency responses of $W(z)$ and $A(z)B(z)$ for the desired noise control frequency band (below 2 kHz).

by filters designed by the traditional high sampling rate method with the original impulse response duration (15 ms). In Fig. 9, the "Normalized PSD" is the power spectral density of the error noise signal divided by the averaged noise power spectral density at error sensors across all frequencies when the ANC system is not in operation (i.e., the "ANC OFF"). It is noted that the traditional high sampling rate method using the original impulse response duration requires 300 multiplications in implementing the real-time filtering process for each sampling interval (50 µs), while the proposed efficient low-delay polyphase method only requires $(40 + 300)/5 = 68$ multiplications for each sampling interval (also in 50 µs) which reduces the real-time computational load to only 23% of that when using the traditional high sampling rate methods. Thus, compared with the traditional high sampling rate method, the proposed method uses much less real-time computations and has almost the same noise control performance. A comparison of real-time multiplications per second for different traditional methods and the proposed method in this experimental setup is shown in Table 2. Note that both "low sampling rate (large delay)" and "high sampling rate (low delay) + shorter impulse

response duration" methods will negatively affect noise control performance which will be confirmed later.

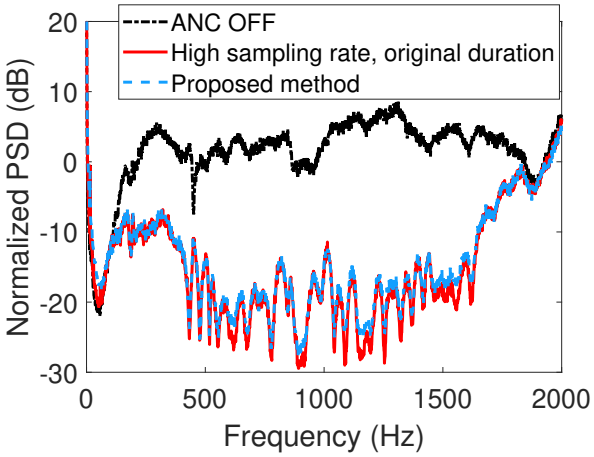

Figure 9: The comparison of noise control performance for traditionally used high sampling rate method using the original impulse response duration and the proposed efficient low-delay polyphase implementation method at the desired noise control frequency band. The proposed method has the same performance but saves 77% real-time computations compared with the high sampling rate method.

In Fig. 10, when using approximately the same real-time computations as the proposed method (i.e., effectively around 60 or 68 multiplications at 20 kHz rate), the noise control performance of the proposed method is better than that of the traditional high sampling rate for 3 ms impulse response duration or low sampling rate method for 15 ms. In Fig. 10, the traditionally used high sampling rate method using shorter impulse response duration has worse noise control performance compared with the proposed method because it uses only a 3 ms impulse response duration which is much shorter compared with around 15 ms. The traditionally used low sampling rate method has almost no noise control performance because, at such a low sampling rate, the introduced electronic delay is too high as already shown in Fig. 7.

The experimental result section confirms that, compared with the low sampling rate method, all two traditional high sampling rate methods and the proposed method can achieve better noise control performance because the use of a high sampling rate reduces introduced electronic delay. The proposed method increases real-time computations linearly with the sampling rate while the traditional high sampling rate method using the original im-

Table 2: A comparison of real-time multiplications per second for different traditional methods and the proposed method in the experimental setup.

Methods	Low f_s method	High f_s method, original impulse response duration	High f_s method, shorter impulse response duration	Proposed method
Sampling Rate f_s	4 kHz	20 kHz	20 kHz	20 kHz
impulse response duration	15 ms	15 ms	3 ms	16.95 ms
Filter Order	60	300	60	340
Real-time Multiplications	240 k	6000 k	1200 k	1360 k
Delay	> 2 ms	< 0.06 ms	< 0.06 ms	< 0.06 ms

pulse response duration increases real-time computations quadratically. In this experimental setup, since the sampling rate is increased to 5 times the original sampling rate, the proposed method reduces to around one-fifth of the multiplications compared with the traditional high sampling rate method using the original impulse response duration. Compared with the traditional high sampling rate method using shorter impulse response duration, i.e., high sampling rate with shortened filter length, the proposed method has much better noise control performance while keeping similar required real-time computations.

4. Conclusion

In real-time implementation of active noise control filters, the electronic delay introduced to the signal path because of the necessary anti-aliasing and reconstruction filters, and ADC and DAC can adversely affect the noise control performance of the ANC system. One common approach to reducing this electronic delay is to use a much higher sampling rate than the desired noise control band. However, the required real-time computations increase quadratically with the sampling rate if the filter is directly implemented in a traditional way. Although the filter length can be shortened to reduce

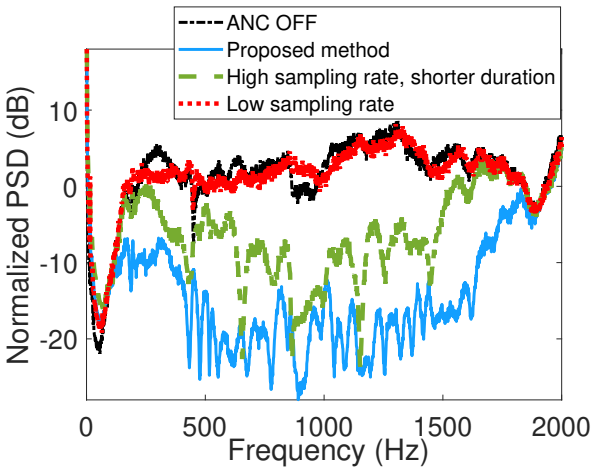

Figure 10: The comparison of noise control performance for the traditional high sampling rate method using shorter impulse response duration, the low sampling rate method, and the proposed efficient low-delay polyphase implementation method at the desired noise control frequency band.

the real-time computations, noise control performance will also be severely affected due to the shortened filter length.

In this article, an efficient low-delay polyphase implementation and the associated multiplicative causal filter decomposition method are proposed. The proposed method uses the property that the frequency response of a high sampling rate ANC filter should be attenuated outside the desired noise control band to prevent noise amplification. Thus, the high sampling rate ANC filter can be decomposed into two multiplicative causal sub-filters by the proposed causal filter decomposition method using a minimum-phase low-pass filter decomposition. The two causal sub-filters can then perform as both control filters and anti-aliasing (and reconstruction) filters so polyphase implementation can be used to reduce the real-time computations without introducing an additional delay. By using the proposed methods, the real-time computations only increase with the sampling rate linearly instead of quadratically. Experimental results confirm that the noise control performance when using the proposed method is not sacrificed compared with using a high sampling rate and implementing a filter in a traditional way whose real-time computations increase with the sampling rate quadratically. After using the proposed method, less electronic delay is introduced to the ANC system and the noise control performance can be enhanced.

A smaller physical dimension of the broadband ANC system is also possible with the proposed method since the reduced delay allows a closer distance between reference microphones, secondary speakers, and the desired noise control region. Broadband ANC may be more applicable in space-limited applications using a reasonable amount of real-time computations. The proposed method also has the potential to be incorporated into the adaptive ANC algorithm (e.g., FxLMS) in both the filtering process and the coefficient updating process. The multiplicative causal filters, $A(z)$, only need to be a pre-designed fixed coefficients maximum-phase lowpass filter without adaptation. Another multiplicative causal filter, $B(z)$, may be trained in real-time using the frequency-domain constrained FxLMS algorithm [27], which can be a future direction of the current work.

5. Acknowledgments

The authors thank Beijing Ancsonic Technology Co. Ltd for providing financial support related to the presented work.

References

[1] Z. Zhang, M. Wu, L. Yin, C. Gong, J. Wang, S. Zhou, J. Yang, Robust feedback controller combined with the remote microphone method for broadband active noise control in headrest, Applied Acoustics 195 (2022) 108815.

[2] Y. Zhuang, X. Wang, Y. Liu, Singular vector filtering method for mitigation of disturbance enhancement in multichannel active noise control systems, Noise Control Engineering Journal 69 (5) (2021) 451–459.

[3] F. An, B. Liu, Cascade biquad controller design for feedforward active noise control headphones considering incident noise from multiple directions, Applied Acoustics 185 (2022) 108430.

[4] Y. Zhuang, Y. Liu, A stable IIR filter design approach for high-order active noise control applications, in: Acoustics, Vol. 5, MDPI, 2023, pp. 746–758.

[5] Y. Zhuang, Y. Liu, A constrained optimal hear-through filter design approach for earphones, in: INTER-NOISE and NOISE-CON congress

and conference proceedings, Vol. 263, Institute of Noise Control Engineering, 2021, pp. 1329–1337.

[6] J. Cheer, S. J. Elliott, Multichannel control systems for the attenuation of interior road noise in vehicles, Mechanical Systems and Signal Processing 60 (2015) 753–769.

[7] S. Kim, M. E. Altinsoy, Active control of road noise considering the vibro-acoustic transfer path of a passenger car, Applied Acoustics 192 (2022) 108741.

[8] H. M. Lee, Y. Hua, Z. Wang, K. M. Lim, H. P. Lee, A review of the application of active noise control technologies on windows: Challenges and limitations, Applied Acoustics 174 (2021) 107753.

[9] P. A. Lopes, J. A. B. Gerald, Low delay short word length sigma delta active noise control, IEEE Transactions on Circuits and Systems I: Regular Papers 68 (9) (2021) 3746–3757.

[10] P. A. Lopes, Low-delay and low-cost sigma-delta adaptive controller for active noise control, Circuits, Systems, and Signal Processing (2022) 1–12.

[11] N. Krishnamurthy, M. Mansour, R. Cole, Implementation challenges for feedback active noise cancellation, in: 2012 IEEE International Conference on Acoustics, Speech and Signal Processing (ICASSP), IEEE, 2012, pp. 1649–1652.

[12] M. R. Bai, Y. Lin, J. Lai, Reduction of electronic delay in active noise control systems—a multirate signal processing approach, The Journal of the Acoustical Society of America 111 (2) (2002) 916–924.

[13] B. Lam, W.-S. Gan, D. Shi, M. Nishimura, S. Elliott, Ten questions concerning active noise control in the built environment, Building and Environment 200 (2021) 107928.

[14] S. Elliott, 10 - hardware for active control, in: Signal Processing for Active Control, Signal Processing and its Applications, Academic Press, London, 2001, pp. 439–465. doi:https://doi.org/10.1016/B978-012237085-4/50012-0.

[15] P. Nelson, S. Elliott, Active control of sound, ACADEMIC PRESS INC., 1994, Ch. 6.13, pp. 194–195.

[16] D. R. Morgan, J. C. Thi, A delayless subband adaptive filter architecture, IEEE transactions on signal processing 43 (8) (1995) 1819–1830.

[17] S. J. Park, J. H. Yun, Y. C. Park, D. H. Youn, A delayless subband active noise control system for wideband noise control, IEEE transactions on speech and audio processing 9 (8) (2001) 892–899.

[18] G. Long, Y. Wang, T. C. Lim, Optimal parametric design of delayless subband active noise control system based on genetic algorithm optimization, Journal of Vibration and Control (2021) 10775463211001625.

[19] J. Cheer, S. Daley, An investigation of delayless subband adaptive filtering for multi-input multi-output active noise control applications, IEEE/ACM Transactions on Audio, Speech, and Language Processing 25 (2) (2016) 359–373.

[20] D. Shi, W.-S. Gan, B. Lam, S. Wen, Feedforward selective fixed-filter active noise control: Algorithm and implementation, IEEE/ACM Transactions on Audio, Speech, and Language Processing 28 (2020) 1479–1492.

[21] D. Shi, B. Lam, K. Ooi, X. Shen, W.-S. Gan, Selective fixed-filter active noise control based on convolutional neural network, Signal Processing 190 (2022) 108317.

[22] J. G. Proakis, D. G. Manolakis, Digital signal processing - principles, algorithms, and applications, 4th Edition, Pearson Prentice Hall, 2007, Ch. 11, pp. 750–813.

[23] Y. Zhuang, Y. Liu, Constrained optimal filter design for multi-channel active noise control via convex optimization, The Journal of the Acoustical Society of America 150 (4) (2021) 2888–2899.

[24] Y. Zhuang, Y. Liu, A numerically stable constrained optimal filter design method for multichannel active noise control using dual conic formulation, The Journal of the Acoustical Society of America 152 (4) (2022) 2169–2182.

[25] G. A. Sitton, C. S. Burrus, J. W. Fox, S. Treitel, Factoring very-high-degree polynomials, IEEE Signal Processing Magazine 20 (6) (2003) 27–42.

[26] L. R. Rabiner, B. Gold, Theory and application of digital signal processing, Englewood Cliffs: Prentice-Hall (1975).

[27] D. Shi, W.-S. Gan, B. Lam, X. Shen, A frequency-domain output-constrained active noise control algorithm based on an intuitive circulant convolutional penalty factor, IEEE/ACM Transactions on Audio, Speech, and Language Processing 31 (2023) 1318–1332.